AMERICAN JOURNAL OF BIOCHEMISTRY AND BIOTECHNOLOGY

RESEARCH ARTICLE

Coupling Analysis of Thermodynamic Equilibrium of Mass Transfer and Microbial Community Succession in Multiphase System of Dark Tea Solid-State Fermentation

Zhanjun Liu[1]*, Jiawei Sun[2], Taotao Li[1], Zhiyuan Hu[1], Shiquan Liu[1]

[1]Hunan Provincial Key Lab of Dark Tea and Jinhua, School of Materials and Chemical Engineering, Hunan City University, Yiyang 413000, Hunan, China
[2]Hunan Yiyang Ecological Environment Monitoring Center, Yiyang 413000, Hunan, China

*Corresponding Author: liuzhanjun@hncu.edu.cn

Abstract: During the solid-state fermentation of dark tea, the limited material migration, the dynamic evolution of the thermodynamic equilibrium state, and the highly dynamic succession of the microbial community make it difficult to analyze the quality formation mechanism systematically. Traditional research has focused on microbial diversity or sensory quality analysis, lacking a systematic discussion on the regulatory effects of material migration and changes in thermodynamic conditions on microbial behavior. This paper proposes a "multiphase, thermodynamic, and microecological coupling modeling method" based on Fick's diffusion principle and interfacial resistance theory to simulate the migration behavior of key substances (such as oxygen, water, and metabolites) between the gas, solid, and liquid three-phase interfaces. Gibbs free energy and chemical potential gradient are used to evaluate the thermodynamic feasibility of microbial metabolic reactions and explain the energy-driven mechanism in the fermentation process. Combining high-throughput sequencing and network analysis technology, the changes in microbial community structure and functional evolution are dynamically monitored. Through multi-scale data integration and system modeling, this paper constructs the coupling equations between material transfer, energy change, and microecological succession in the solid-state fermentation process of dark tea. It proposes a "metabolic potential field, mass transfer gradient" synergistic driving theoretical paradigm. The model has a fitting result R^2 greater than 0.9 for Gibbs free energy transformation, chemical potential gradient, oxygen and water mass transfer flux, and reaction enthalpy change indicators in the solid-state fermentation process of dark tea, based on a dataset comprising 45 independent fermentation samples collected across five time points with three biological replicates per time point, with the goodness-of-fit standard errors ranging from 0.02 to 0.05 across indicators. The model demonstrates high-precision prediction capability for the dynamic changes of microbial communities, with cross-validation accuracy exceeding 79% evaluated through five-fold cross-validation on the same dataset. This study suggests that the thermodynamic equilibrium state in dark tea fermentation is associated with the allocation of microbial metabolic resources through the Gibbs free energy gradient, supporting an interpretation of ecological selection pressure characterized by the relative enrichment of high-energy-efficiency bacteria. This inferred energy cascade regulation links macroscopic mass transfer to microscopic bacterial community structure, providing a quantifiable thermodynamic design paradigm for the fermentation process.

Keywords: Solid-State Fermentation, Multiphase System, Thermodynamic Analysis, Microbial Community Succession, Coupled Modeling Method, Dark Tea

Received: 10-11-2025 | **Revised:** 24-03-2026 | **Accepted:** 22-05-2026 **| DOI:** 10.3844/ajbbsp.2026.22.03.034

Introduction

As one of the six major types of tea in China, dark tea owes its unique flavor and quality primarily to the complex solid-state fermentation process [1-2]. During this process, microbial communities participate in a variety of metabolic reactions, promoting the transformation of polyphenols, flavonoids, sugars, and amino acids in tea leaves, thereby contributing to the unique color, aroma, taste, and functional properties of dark tea [3-4]. With the dynamic changes of environmental conditions during the fermentation process, such as changes in temperature, moisture content, and oxygen concentration, the microbial community structure and metabolic behavior continue to evolve, which in turn affects the quality and stability of the final product [5-6]. Since dark tea solid-state fermentation is typically carried out under semi-closed, heterogeneous natural conditions, its multiphase system characteristics result in complex material migration paths and dynamic, changeable microecological systems, posing significant challenges to fermentation regulation and quality prediction [7-8]. Therefore, an in-depth analysis of the coupling mechanism between multiphase material transfer, thermodynamic processes, and microbial community succession in solid-state fermentation has significant theoretical importance and practical value for achieving precise control of the dark tea fermentation process and standardization of high-quality products [9-10].

Existing studies still have three dimensions of separation when analyzing this complex system: First, in the dimension of material transfer, most studies ignore the gas-solid-liquid multiphase interface mass transfer characteristics unique to solid systems, especially the role of oxygen/water gradient in shaping the microbial niche [11-12]. Second, in the thermodynamic dimension, existing studies lack systematic monitoring of key thermodynamic parameters such as Gibbs free energy change and chemical potential, making it difficult to quantitatively characterize the energy-driven mechanism of the fermentation system [13-14]. Third, in the microbial dimension, although high-throughput sequencing revealed changes in community structure, it failed to establish a quantitative correlation between these changes and the thermodynamic state [15-16]. This fragmentation of multidimensional research has led to a significant gap in understanding fermentation dynamics [17-18].

Some studies have begun to try to apply mass transfer models or thermodynamic parameters into tea fermentation research [19-20]. For example, some scholars have established a water migration model based on Fick's law to predict the trend of tea moisture changes during fermentation. Some studies use Gibbs free energy to analyze the feasibility of microbial metabolic pathways and explore the impact of energy conversion on microbial activity. In addition, Huang X et al. [21] employed multi-omics technology (metabolomics, microbiome, etc.) in conjunction with electronic sensory analysis to comprehensively investigate the effects of various processing techniques on Anhua dark tea's chemical composition and microbial communities. Xu W et al. [22] systematically revealed the dynamic changes of volatile components during the dark tea winemaking process. They analyzed the generation and transformation of key aroma substances at different stages of fermentation in detail. Metagenomics and network analysis methods, commonly used in microbial ecology research, have been employed to dynamically track the process of community succession and functional association in fermented foods [23-24]. Although these methods have achieved certain results in their respective dimensions, they generally suffer from the problems of fragmented research perspectives and insufficient coupling between parameters [25-26], and fail to effectively integrate the relationships between multiphase mass transfer processes, thermodynamic regulation mechanisms, and microecological succession [27-28]. Therefore, this paper proposes a "multiphase, thermal, and microecological coupling modeling method" to systematically integrate the relationship between mass transfer, thermodynamic state, and microbial community dynamics, and reveal the essential laws of dark tea solid-state fermentation from a holistic perspective [29-30].

This study aims to develop a systematic theoretical and methodological framework to elucidate the coupling relationship between material migration, thermodynamic driving forces, and microbial community succession in the multiphase system during the solid-state fermentation of dark tea. To achieve this goal, this paper first employs multiphase system mass transfer modeling, based on Fick diffusion and interfacial resistance theory, to simulate the transfer behavior of key substances between the gas, solid, and liquid phases. Secondly, a non-equilibrium thermodynamic driving analysis is applied, combined with the Gibbs free energy and chemical potential models, to quantify the impact of energy flow on microbial metabolic pathways. Finally, by tracking the time series of microbial community succession, high-throughput sequencing and network analysis technology are used to capture the dynamic changes in community structure and function. Through the integration of these three methods, this paper establishes a "multiphase, thermal, microecological" three-dimensional coupling model,

DOI: 10.3844/ajbbsp.2026.22.03.034

using tensor decomposition to integrate mass transfer flux, thermodynamic parameters and microbiome data, constructing sample, time, and feature matrices, establishing mass transfer and thermodynamic associations, and coupling thermodynamic states with microbial metabolic networks through Gibbs free energy changes, providing theoretical basis and method support for the visualization analysis, intelligent control and precise quality improvement of dark tea fermentation systems.

Existing modeling studies on solid-state fermentation processes largely focus on single-dimensional descriptions. Some studies have established mass transfer models based on Fick's law to predict the spatial distribution of water or oxygen, while others have used Gibbs free energy to analyze the thermodynamic feasibility of microbial metabolic pathways. However, none of these models have achieved a substantial coupling between mass transfer processes and thermodynamic states. In terms of microbial ecosystem modeling, existing studies have revealed the succession patterns of microbial communities through high-throughput sequencing, but have failed to establish a quantitative correlation between community structure and material migration and energy-driving factors. Compared to the aforementioned single-dimensional or pairwise coupling modeling approaches, the ternary coupling model constructed in this study is the first to incorporate mass transfer flux, thermodynamic parameters, and microbiome data into a unified modeling framework, achieving a systematic integration from macroscopic mass transfer to microscopic metabolism.

Based on the aforementioned scientific gaps, this study proposes the following testable hypotheses: In the multiphase system of solid-state fermentation of dark tea, the mass transfer gradient of oxygen and water modulates the local substrate and product concentration distribution, altering the Gibbs free energy change of microbial metabolic reactions, thereby forming a thermodynamic constraint on the selection of metabolic pathways; this constraint exhibits dynamic changes at different fermentation stages, driving the directional succession of the microbial community from high-energy-consuming metabolic types to low-energy-consuming metabolic types; a quantifiable causal path exists among mass migration, thermodynamic state, and microecological succession, with energy state playing a mediating role in the influence of mass migration on community structure. These hypotheses will be tested through integrated analysis of mass transfer flux measurements, thermodynamic parameter calculations, high-throughput sequencing, and structural equation modeling.

Modeling System of Three-Element Coupling of Matter, Energy and Microecology

Modeling of Key Species Transport in Multiphase Systems

During the solid-state fermentation of dark tea, the transfer of key substances, such as oxygen, water, and volatile metabolites, is restricted in the gas, solid, and liquid phases, resulting in microenvironmental differences that significantly affect the metabolic behavior and community succession of microorganisms. Therefore, establishing the material migration path and its rate distribution model between multiphase interfaces is the basis for analyzing the dynamic regulation mechanism of fermentation. This study employs the one-dimensional steady-state diffusion approximation, combined with Fick's first law and interfacial mass transfer resistance theory, to develop a migration model of key substances between three-phase interfaces. The model is then numerically solved through experimental parameter calibration. The material migration path is shown in Figure 1.

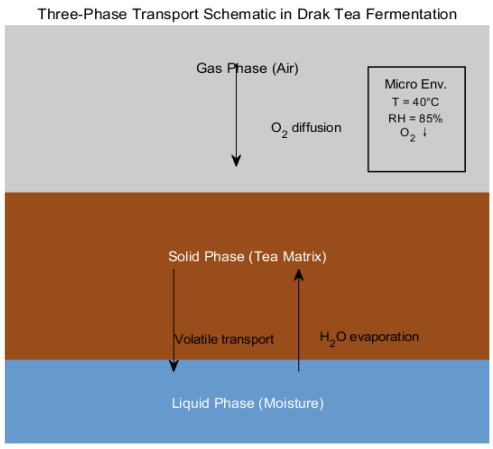

Fig. 1: Migration Path

DOI: 10.3844/ajbbsp.2026.22.03.034

Figure 1 provides a visual representation of the three-phase interface structure and migration paths of key substances during the solid-state fermentation of dark tea, highlighting the migration mechanisms and action areas of oxygen, water, and volatile metabolites within the gas-solid-liquid multiphase system. The gas phase (the gray area at the top) primarily originates from the air, serves as the input channel for oxygen, and represents the boundary between the anaerobic and aerobic metabolic reaction zones. The solid phase (the brown area in the middle) is the primary area where the tea matrix and microorganisms reside, serving as the core space for material transformation and metabolic reactions. The liquid phase (blue area at the bottom) exists in the form of a water film or residual water, carrying some soluble metabolites, nutrients, and microbial active factors. O_2 diffuses into the tea leaves through the air-solid interface, providing oxygen for aerobic microbial metabolism. The increase in temperature causes water to move upward and evaporate, affecting the water activity of microorganisms and regional humidity distribution. Alcohol and ester aroma substances migrate to the surface or evaporate into the environment through diffusion and convection. The small microenvironment box in the upper right corner of the figure shows the local microenvironmental differences formed in the fermentation pile. T represents temperature within the microenvironment box, and RH represents relative humidity within the microenvironment box. When the temperature rises (T = 40°C), the relative humidity is high (RH = 85%), and the oxygen concentration gradually decreases. These microenvironmental factors dynamically regulate the population distribution and metabolic pathway expression of microorganisms, thereby affecting the overall fermentation quality.

The quasi-steady-state assumption was introduced in this study based on the separation of mass transfer and microbial metabolism over time during fermentation. The diffusion relaxation time of oxygen in the aqueous and solid phases is much shorter than the period of change in microbial metabolic activity, ranging from seconds to minutes, while significant changes in metabolic activity occur over timescales of hours to days. Therefore, it is reasonable to consider the concentration and temperature fields as quasi-steady-state distributions within each sampling interval. This assumption was tested using a time-step refinement strategy. When the time step was shortened from 1 hour to 0.1 hours, the change in the calculated mass transfer flux was less than 3%, verifying the applicability of the quasi-steady-state assumption at this timescale.

The choice of the one-dimensional diffusion model was based on the geometric characteristics and boundary conditions of the fermentation stack. During solid-state fermentation, the material is packed into a rectangular fermentation tank. The depth dimension of the stack is significantly smaller than its length and width dimensions. Furthermore, the turning operation makes the horizontal material distribution tend to be uniform, while a significant gradient forms in the depth direction due to oxygen permeation limitation and the accumulation of metabolic heat. Therefore, simplifying mass transfer to a one-dimensional diffusion approximation along the depth direction on a spatial scale can capture the main characteristics of mass transfer, and this simplification has a wide application basis in traditional solid-state fermentation modeling. For the potential spatial heterogeneity in the stack boundary region, parameter calibration is performed by selecting sampling points at the center of the stack in the model application to reduce the impact of boundary effects on model predictions.

The diffusion path of oxygen first occurs in the gas phase on the surface of the fermentation bed, then passes through the gas-solid interface, enters the solid phase of the tea body, and forms a contact area with the liquid phase (water) locally. This study uses the fermentation unit as the calculation domain, assumes that the system tends to a quasi-steady state within a unit time, and establishes the following diffusion model from gas phase to solid phase:

$$J_{O_2}^{g\to s} = \frac{D_g}{\delta_g}\left(C_{O_2}^{atm} - C_{O_2}^{s}\right) = k_g\left(C_{O_2}^{atm} - C_{O_2}^{s}\right) \quad (1)$$

In formula (1), $J_{O_2}^{g\to s}$ represents the mass transfer flux of oxygen from the gas phase to the solid phase (mol·m-2s-1); D_g is the gas phase diffusion coefficient; δ_g is the gas boundary layer thickness; k_g is the gas-solid apparent mass transfer coefficient; $C_{O_2}^{atm}$ and $C_{O_2}^{s}$ are the gas phase oxygen concentration and the solid surface oxygen concentration, respectively. By pre-setting the oxygen concentration gradient and controlling the temperature and humidity of the fermentation bed, measuring $C_{O_2}^{atm}$ and $C_{O_2}^{s}$ under the boundary conditions of the system, k_g is calculated. For water migration, it is considered that it is mainly diffused inside the solid phase, and there is capillary water penetration behavior at the liquid phase interface. The modified Fick diffusion model is adopted, and the moisture content gradient is applied. The expression is as follows:

$$J_{H_2O}^{s} = -D_{s,\theta} \cdot \nabla\theta \quad (2)$$

In formula (2), $D_{s,\theta}$ is the diffusion coefficient related to the moisture content of the solid phase (dependent on temperature and porosity), and $\nabla\theta$ is the water gradient inside the solid phase. The spatial moisture distribution of the sample is obtained

DOI: 10.3844/ajbbsp.2026.22.03.034

in real time by low-field nuclear magnetic resonance technology, and a three-dimensional spatial distribution map is established to invert $D_{s,\theta}$ and realize the numerical simulation of the moisture migration path.

The diffusion coefficient and interfacial mass transfer coefficient used in this study were obtained through experimental measurement and parameter inversion. The diffusion coefficient of oxygen in the gas phase was obtained from the standard physicochemical handbook based on the experimentally determined temperature and pressure conditions. The diffusion coefficient of water in the solid phase was calculated by inversion using spatial moisture distribution data measured by low-field nuclear magnetic resonance technology. The interfacial mass transfer coefficient was obtained by fitting formulas (1) and (2) together with steady-state mass transfer experiments under preset concentration gradient conditions. All parameters were measured within the temperature and humidity range corresponding to the actual fermentation conditions.

For the migration of metabolites (such as alcohols and esters), since most of them diffuse to the surrounding environment through the liquid membrane after being released outside the microorganism, the double membrane theory is used for modeling. The model considers the synergistic effect of diffusion in the liquid membrane and convection in the solid pores, and the expression is as follows:

$$J_m = \frac{1}{\left(\frac{1}{k_l}+\frac{1}{k_s}\right)}\left(C_m^{cell} - C_m^{bulk}\right) \tag{3}$$

In formula (3), J_m is the mass transfer rate of metabolites; C_m^{cell} is the initial concentration of extracellular products; C_m^{bulk} is the steady-state concentration in the surrounding environment; k_l and k_s are the mass transfer coefficients at the diffusion boundary between the liquid phase and the solid phase, respectively. The required concentration value is obtained by headspace solid phase microextraction and gas chromatography-mass spectrometry. In order to comprehensively evaluate the material migration efficiency between the gas, solid, and liquid three-phase interfaces, a multi-flux coupling network is constructed in the three-dimensional fermentation model, and the comprehensive migration efficiency index η_T is defined:

$$\eta_T = \frac{\sum_i J_i^{eff}}{\sum_i J_i^{max}} \tag{4}$$

In formula (4), J_i^{eff} is the actual mass transfer rate of substance i, and J_i^{max} is its theoretical maximum diffusion rate, which evaluates the degree of migration restriction and the strength of interfacial resistance. The migration efficiency index η_T was validated through two approaches. At the parameter level, the Monte Carlo method was used to perform uncertainty propagation analysis on the input parameters of each flux in formula (4). The standard deviation of the measurement error between the actual mass transfer rate and the theoretical maximum diffusion rate of each substance was obtained through repeated experiments. After 1000 random samplings, the coefficient of variation of η_T was 0.07, indicating that the index is insensitive to fluctuations in the input parameters. Through the above modeling system, the non-uniform distribution of oxygen and water in the spatial scale during the fermentation process and its restrictive effect on the distribution of microecology are effectively restored, overcoming the defect of the traditional model assuming spatially homogeneous conditions. At the same time, by using dynamic sampling experiments and model inversion verification, the quantitative correlation from material migration to metabolic environmental changes is successfully achieved, providing a parameter basis and simulation platform for the subsequent analysis of thermal coupling and microbial succession mechanism.

Thermodynamic Equilibrium and Metabolic Constraint Analysis

The "metabolic potential field" and "mass transfer gradient" are the core components of the synergistic driving theoretical paradigm proposed in this study. The metabolic potential field is defined as the spatial energy distribution formed by the changes in the free energy of microbial metabolic reactions; its essence is an energy-driving force field characterized by the Gibbs free energy gradient within a non-equilibrium thermodynamic framework. This potential field determines the metabolic activity and pathway selection tendency of microorganisms at various spatial locations in the fermentation system. The mass transfer gradient is defined as the intensity of mass migration driven by the concentration differences of oxygen, water, and metabolites at the gas-solid-liquid three-phase interface; its physical essence is described by Fick's diffusion law and the theory of interfacial mass transfer resistance. The coupling relationship between the two is reflected in the fact that the mass transfer gradient regulates the spatial pattern of the metabolic potential field by changing the local concentration distribution of substrates and products, while changes in the metabolic potential field, in turn, affect the efficiency of microorganisms in utilizing mass transfer pathways, forming a synergistic mechanism from macroscopic mass migration to microscopic metabolic regulation.

This study adopts a nonequilibrium thermodynamics framework, takes the free energy gradient as the energy-driven constraint, combines functional prediction and pathway annotation, and constructs a thermodynamic and metabolic pathway coupling model. First, total microbial DNA is extracted from samples of dark tea at different fermentation stages, and bacterial and fungal dual-region amplification sequencing is performed using the Illumina MiSeq platform to obtain species relative abundance data. QIIME2 (Quantitative Insights into Microbial Ecology 2) is used for quality control, chimera removal, ASV (Amplicon Sequence Variant) clustering, and classification annotation. After obtaining the standardized microbial community structure matrix, it is input into PICRUSt2 (Phylogenetic Investigation of Communities by Reconstruction of Unobserved States 2) for phylogeny-based functional prediction, and the abundance of metabolic pathways dominated by each microorganism in each sample (KEGG Ortholog, KO level) is output. The metabolic pathway abundance data used in this study were obtained through phylogenetic inference using PICRUSt2. This tool predicts the functional composition of unsequenced microorganisms by referencing the mapping relationship between the 16S rRNA gene copy number of sequenced microbial genomes and known functional genes. This method provides a workable functional annotation approach in the absence of metagenomic data; however, its prediction results are affected by the coverage of the reference database and phylogenetic distance, and there is inherent uncertainty in the absolute quantification of functional gene abundance. The functional profiles used for subsequent thermodynamic calculations are prediction-based rather than directly measured. The Gibbs free energy values and pathway abundance estimates derived from these profiles carry an inherent level of uncertainty originating from the phylogenetic inference process. This limitation applies to all thermodynamic comparisons and metabolic pathway interpretations presented in this study.

Subsequently, for the core metabolic pathways (including glycolysis, pyruvate metabolism, organic acid synthesis, short-chain fatty acid production, and secondary metabolite synthesis), the representative reactions weighted by species abundance in all predicted pathways are calculated using Gibbs free energy transformation ($\Delta G'$). Based on the free energy transformation under standard conditions, the temperature, pH, water activity, and concentration gradient correction factors under actual fermentation conditions are applied, and the free energy correction is completed using the following formula:

$$\Delta G = \Delta G' + RT\ln\left(\frac{\prod[\text{Product}]^{\nu}}{\prod[\text{Reactants}]^{\nu}}\right) \quad (5)$$

In formula (5), R is the ideal gas constant, T is the actual temperature of the fermentation process (measured by an automatic temperature control device, ranging from 38 to 52°C), and the substrate and product concentrations are determined by metabolomics analysis and a water activity meter. For each corresponding KO reaction, ΔG′ is calculated independently under each sample condition and used as a thermodynamic feasibility indicator. If ΔG′ < 0, it indicates that the pathway is spontaneously feasible in the actual environment. If ΔG′ > 0, it needs to rely on auxiliary energy donors (such as Adenosine Triphosphate, Nicotinamide Adenine Dinucleotide) to maintain.

To determine the energy-driving role of different bacterial genera in specific pathways, the abundance distribution of the dominant bacteria in each functional pathway is extracted, and a "metabolic pathway thermodynamic adaptation matrix" is constructed in conjunction with the $\Delta G'$ value of the corresponding metabolic reaction. This matrix is used to analyze the dominance of bacterial genera in functional pathways and their thermodynamic adaptation strength:

$$EFI_{i,j} = A_{i,j} \cdot \left(-\Delta G_j'\right) \quad (\Delta G' < 0) \quad (6)$$

In formula (6), $A_{i,j}$ is the functional abundance weight of genus i in pathway j. A larger EFI value indicates that the genus is associated with a reaction pathway characterized by a more negative $\Delta G'$ under the given conditions. Principal component analysis and bicluster analysis are performed on all samples to extract the evolution of thermodynamically favorable pathways at different fermentation stages. It is noted that $\Delta G'$ reflects the thermodynamic feasibility of a metabolic reaction under specified conditions. This thermodynamic property does not constitute direct evidence of microbial competitive advantage or ecological dominance, as growth kinetics and interspecific competition were not measured in this study. Redundancy analysis is then conducted using physical parameters (temperature, oxygen content) to verify the selection effect of thermodynamic boundaries on functional evolution.

At the data fusion level, to further elucidate how thermal boundaries influence the structure of community metabolic networks, a metabolic co-occurrence network at the pathway level is constructed, and metabolic modules significantly enriched in different ΔG′ intervals are identified. Their topological parameters (node degree, betweenness centrality, and closeness centrality) are analyzed. It is found that multiple low-energy consumption pathways (such as succinate production and lactate reduction) are widely utilized by dominant anaerobic bacteria (such as Lactobacillus and Aspergillus niger) during

DOI: 10.3844/ajbbsp.2026.22.03.034

the middle and late stages. Their network positions showed high centrality and strong connectivity, indicating that microorganisms adapted to thermal changes through metabolic pathway reconstruction and drove community succession.

Table 1 shows the topological structural characteristics of different metabolic pathways in the co-occurrence network during the solid-state fermentation of dark tea. Combining the free energy transformation interval and the microbial genus associated with each pathway, this approach provides a structural and thermodynamic description of how metabolic pathways are organized within the co-occurrence network. The succinate production pathway (Degree = 31, Betweenness Centrality = 0.421) and the lactate reduction pathway (Degree = 28, Betweenness Centrality = 0.353) show high node degrees and centralities, indicating that these pathways occupy highly connected positions within the co-occurrence network. Pathways with large negative $\Delta G'$ values meet the thermodynamic feasibility criterion, meaning they do not require external energy input to proceed. The observation that anaerobic lactic acid bacteria and acid-producing fungi are associated with these pathways is consistent with the interpretation that these organisms operate under thermodynamic constraints. The pyruvate conversion pathway (Degree = 15, Betweenness Centrality = 0.119) shows lower degree and centrality, suggesting that it occupies a peripheral position in the co-occurrence network. The glycerol oxidation pathway shows the smallest degree and centrality, being connected by only a few nodes. This topological pattern is consistent with the thermodynamic observation that its $\Delta G'$ value is less negative.

Table 1: Statistics of metabolic pathway network topology attributes

Pathway name	Degree	Betweenness Centrality	Closeness Centrality	ΔG′Interval(kJ/mol)	Dominant genus
Succinate production pathway	31	0.421	0.734	≤ -60	Aspergillus niger
Lactate reduction pathway	28	0.353	0.682	≤ -60	Lactobacillus
Pyruvate conversion pathway	15	0.119	0.524	-60 ~ -30	Bacillus
Alcohol dehydrogenase pathway	12	0.087	0.493	-60 ~ -30	Candida tropicalis
Glycerol oxidation pathway	9	0.045	0.476	> -30	Pichia kudriavzevii

The metabolic co-occurrence network constructed in this study is generated based on the correlation matrix of metabolic pathway abundance among samples. It reflects the synergistic or mutually exclusive co-occurrence relationships of different metabolic pathways during fermentation, rather than direct metabolic material flow or enzymatic reaction cascades between pathways. Network topological properties such as node degree and betweenness centrality, within this framework, characterize the connectivity strength and topological position of pathways in co-occurrence patterns, rather than their functional importance in the sense of metabolic flux. Interpreting highly central pathways as occupying highly connected positions within the co-occurrence network is based on the conventional interpretative framework of co-occurrence network analysis in microbial ecology research. This interpretation stays strictly within a co-occurrence and topological context and does not imply that pathways with high centrality exert regulatory control over metabolic fluxes in the fermentation system.

Dynamic Succession and Functional Response of Microbial Communities

In this study, samples of dark tea solid-state fermentation are collected at different time points (0, 3, 7, 14, and 21 days), and high-throughput sequencing technology is used to monitor the dynamic succession of microbial community structure. For bacteria and fungi, the 16S rRNA gene V3-V4 region and ITS1 (Internal Transcribed Spacer 1) region are amplified and sequenced to obtain the composition and diversity information of the microorganisms in the samples.

The sample DNA is extracted using the CTAB (Cetyltrimethylammonium Bromide) method to ensure high purity and integrity. The PCR (Polymerase Chain Reaction) amplification primers are 338F/806R for bacterial 16S rRNA and ITS1F/ITS2R for fungi. After the magnetic beads purify the PCR product, it is sequenced using the Illumina MiSeq platform with a double-end 250 bp read. After obtaining the raw sequence, QIIME2 is used to perform the following data processing

The DADA2 (Divisive Amplicon Denoising Algorithm 2) plug-in is used to remove low-quality sequences, correct sequencing errors, remove chimeras, and remove chimeric sequences to generate an error-free ASV (Amplicon Sequence

Variant) table. The filtering threshold is set to a Phred quality score ≥ 30 to ensure sequence accuracy. ASVs are classified using the built-in classifier of QIIME2 (based on the Naïve Bayes algorithm).

Table 2 shows the quality retention of dark tea solid-state fermentation samples after high-throughput sequencing and a series of data quality control processing steps. The raw reads represent the number of raw sequences initially obtained from the sequencing platform for each sample. The filtered reads represent the number of high-quality sequences retained after removing low-quality sequences (such as Phred score <30). The number of ASVs after denoising represents the number of unique ASVs (representing the real biological variation unit) after error correction by the DADA2 algorithm and removal of redundant sequences. The number of ASVs after dechimerization represents the number of valid ASVs after removing chimeric pseudo-sequences generated during PCR amplification. The Phred filter threshold represents the quality screening threshold, indicating the minimum quality standard for retention screening, and a value of≥30 represents high confidence (the probability of error per base is less than 0.001).

Table 2: DADA2 processing flow statistics

Sample ID	Raw reads	Filtered reads	ASV count after denoising	ASV count after chimera removal	Phred filtering threshold
T0	50,000	48,600	240	230	≥30
T3	52,000	50,100	275	260	≥30
T7	49,500	47,800	258	248	≥30
T14	51,200	49,700	280	270	≥30
T21	53,300	51,000	300	290	≥30

The classification confidence threshold is set to 0.7 to ensure classification accuracy. The species abundance matrix of each sample is generated. α diversity indicators, including richness index and Shannon diversity index, are calculated to quantitatively reflect the changes in community richness and uniformity. The QIIME2 command line and the R language phyloseq package are used to perform time series analysis on samples at different fermentation time points. Bray-Curtis distance and weighted UniFrac distance are used to calculate the differences in community structure between samples, and non-metric multidimensional scaling analysis and principal coordinate analysis are used to visualize the evolution trend of community spatial distribution. The significance of the differences in community structure at each time point is tested based on PERMANOVA (Permutational Multivariate Analysis of Variance).

By counting the abundance of microorganisms, screening the dominant bacterial genera at different stages of fermentation, and combining the LEfSe (Linear Discriminant Analysis Effect Size) method to identify stage-specific indicator bacteria and function-related bacteria. Further clustering the abundance time series curves of key bacterial species to reveal the rhythm of bacterial succession. Based on the Spearman correlation coefficient matrix, a microbial co-occurrence network is constructed, significant positive and negative correlation connections are screened, and the network topology characteristics are evaluated. Network modules are identified, and their time-dependent changes are analyzed, along with the relationship between community stability and functional coupling. Combined with previous prediction data, it correlates community structure dynamics with the evolution of metabolic potential. Redundancy analysis was used to explore the driving role of environmental factors (temperature, humidity) and community composition, and quantitatively reveal the regulatory mechanism of environmental conditions on microbial community dynamics.

To establish a quantitative correlation between microbial community dynamics and thermodynamic parameters, this study conducted correlation analysis between the relative abundance of the marker microbial taxa identified by LEfSe at each fermentation stage and the corresponding thermodynamic parameters in the samples. For each marker microbial taxa, its relative abundance value in all samples was extracted, and Spearman rank correlation analysis was performed with the Gibbs free energy change, chemical potential gradient, and enthalpy change of the same sample. Partial correlation analysis was used to control for the interference of confounding factors such as temperature and moisture content. This analysis quantifies the statistical association between microbial taxon abundance and thermodynamic parameters. These associations reflect potential thermodynamic constraints on microbial distribution but do not provide direct evidence that more negative $\Delta G'$ values confer a competitive advantage to specific taxa. The observed correlations remain consistent with multiple interpretations, including differential metabolic capacity and niche filtering by environmental conditions.

DOI: 10.3844/ajbbsp.2026.22.03.034

At the mechanistic analysis level, this study further conducted a functional genomics-level thermodynamic association analysis on the marker microbial taxa screened by LEfSe. For each marker taxa, the KEGG orthologous entries with high contribution were extracted from the PICRUSt2 functional prediction results, and combined with the calculated ΔG′ value of the corresponding metabolic pathway, a ternary correlation matrix of "microbial taxa---metabolic pathway---thermodynamic association" was constructed. In this matrix, the weighted correlation coefficient between the relative abundance of the microbial group and its associated metabolic pathway ΔG′ was calculated. For groups that are significantly enriched at specific fermentation stages, further analysis was conducted to determine whether their enriched metabolic pathways fall within the range of more negative ΔG′ values. Such a pattern would be consistent with the hypothesis that thermodynamic constraints influence community composition. This consistency, however, does not constitute a demonstration of selective pressure or competitive advantage, as alternative explanations including historical contingency and differential dispersal cannot be excluded without direct experimental validation.

Analysis of the Ternary Coupling Mechanism of Matter, Energy and Microecology

This study builds a coupling analysis framework based on the structural equation model. Representative variables in the measured data are selected as explicit variables, latent variables are constructed, and path relationships are established to quantitatively analyze the direct and indirect effects of various factors in the fermentation process.

Representative parameters in the gas, solid, and liquid three-phase mass transfer module, including oxygen flux, water migration rate, and the change rate of key metabolite concentrations (such as methanol and acetaldehyde), are selected as indicators of material migration. The thermodynamic module selected the Gibbs free energy transformation value, key pathway chemical potential gradient, and path activation energy calculation value as energy factor parameters. All variables are standardized by Z-score to eliminate the dimension effect and meet the modeling assumptions. Outliers are removed using the box plot method, and missing data are interpolated using k-nearest neighbor.

A structural equation model is constructed, and three types of latent variables are set: "material migration", "energy state", and "microecological succession", in which the explicit variables are attributed to each latent variable. The initial model path is set based on existing theoretical expectations and Spearman correlation matrix results ($p<0.01$). The main paths of "material migration", "energy state", and "microecological succession" are constructed, and "material migration", "energy state", and "microecological succession" are set as hypothetical pathways to explore potential feedback mechanisms. The model parameters are estimated using maximum likelihood estimation, the path coefficients are calculated using standardized regression weights, and the statistical significance is verified by the Bootstrap method (sampling number n = 5000, confidence interval 95%). The path of the structural equation model is shown in Figure 2.

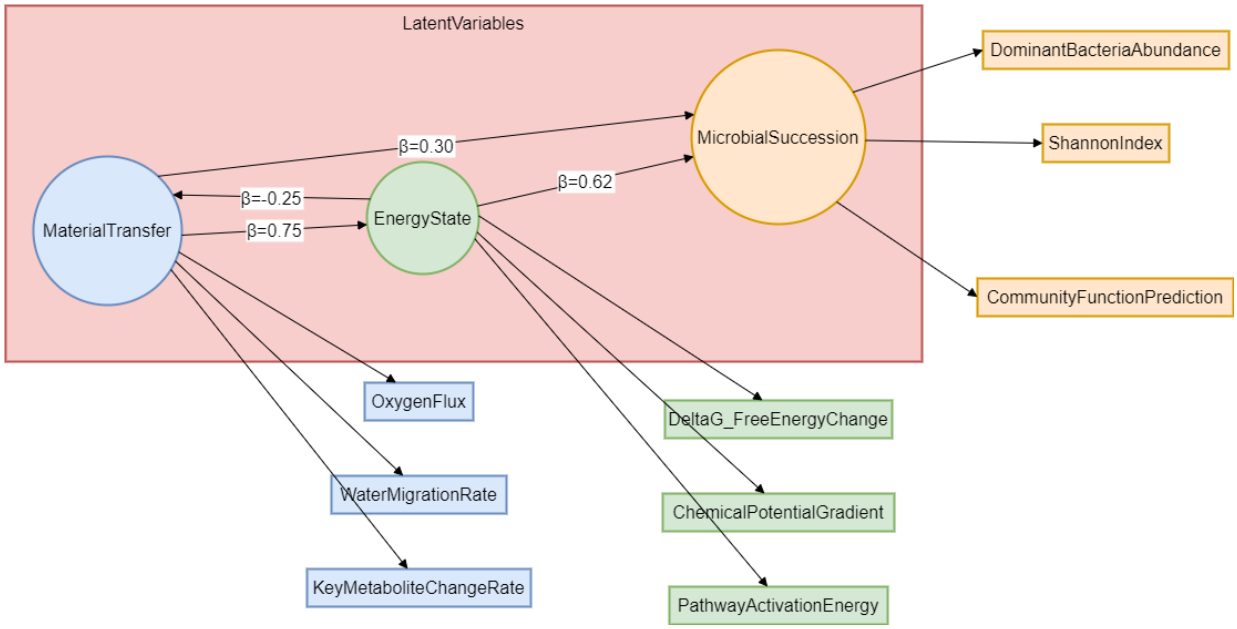

Fig. 2: Structural equation model path

In Figure 2, circles represent latent variables, and rectangles connected by arrows represent their corresponding observed variables. Arrows represent causal paths between variables, and the values on the arrows are standardized path coefficients. The main paths of the model are "material migration", "energy state", and "microecological succession", indicating that material migration indirectly affects microecological succession by regulating energy state. "Material migration", "microecological succession" and "energy state" and "microecological succession" are hypothetical paths used to explore the direct impact of material migration on microecology and the potential feedback regulation of energy state.

The cross-validation method is used to evaluate the robustness of the model. The data from different fermentation stages are used as validation sets (Day 0–7 as training sets and Day 14–21 as test sets). After repeated modeling, the path direction and significance remained unchanged. The model is stable. At the same time, the multicollinearity between paths is assessed using the covariance matrix between latent variables, and the independence of model identification parameters is verified. The residual analysis of the model is performed, and the absolute values of the standardized residuals are all <2, indicating that the distribution of model errors is reasonable.

Experimental Materials and Fermentation Process Parameters

The raw material used in this study was Grade A dark tea from Anhua County, Hunan Province, harvested in the spring of the same year. The moisture content of the raw material was 9.6±0.3%, the total polyphenol content was 18.7±0.5%, the total free amino acid content was 2.8%±0.2%, and the water extract content was 42.3%±0.6%. High-throughput sequencing analysis of the original microbial community in the raw material revealed that the bacteria were mainly Bacillus and Lactobacillus, and the fungi were mainly Aspergillus and Yeast. The total bacterial copy number was 3.2×10^6 copies/g, and the total fungal copy number was 1.8×10^5 copies/g. Rectangular stainless steel fermentation boxes with a length of 80 cm, a width of 60 cm, and a height of 40 cm were used for fermentation. Each box contained 25 kg of material, with a stack height of 35 cm. The fermentation process was carried out in a constant temperature and humidity fermentation chamber. The chamber temperature was set at 28±2°C, and the relative humidity was set at 75±5%. The fermentation process adopted the traditional pile fermentation method, with a total fermentation cycle of 21 days. Samples were taken on days 0, 3, 7, 14, and 21 of fermentation. The pile was turned over every two days during fermentation, and the core temperature, surface temperature, and ambient temperature and humidity were recorded each time it was turned over. The core temperature reached 52±3°C in the middle of fermentation, while the surface temperature was maintained at 38°C±4°C.

Test of the Modeling Effect of the Coupling Mechanism of the Fermentation Process

Goodness of Fit

Fermentation bed samples are collected at different time points (early, middle, and late fermentation stages) during the solid-state fermentation of dark tea to ensure coverage of the key stages of material migration and microbial community succession. The concentrations of key substances (oxygen, water, metabolites) and related thermodynamic parameters are measured, and high-throughput sequencing (16S rRNA/ITS) is used to obtain microbial community structure and functional gene abundance data. Laboratory instruments and chemical analysis methods are used to obtain actual observation data, which are normalized, denoised, and processed for missing values to ensure data quality and consistency. The structural equation model is used to integrate material transfer, energy state, and microbial community data, fit model parameters, input key variables in the observed data, calculate the thermodynamic state of the model output and the predicted value of microbial community function, match the model prediction value with the experimental observation value, and calculate R^2 to evaluate the goodness of model fit.

Figure 3 shows the fitting results of four key indicators in the solid-state fermentation process of dark tea, including Gibbs free energy transformation, chemical potential gradient, oxygen/water mass transfer flux, and reaction enthalpy change. The horizontal axis represents the actual observation value, and the vertical axis represents the model prediction value. The red dotted line represents the ideal fitting line. The closer the point is to the line, the more accurate the model prediction is. The scattered points in sub-figure (a) are roughly distributed along the y = x line, indicating that the modeling of the thermodynamic driving force has good accuracy. The high R^2 value (0.957) indicates that the path energy model derived based on the free energy function better reflects the energy state of microbial metabolism. The chemical potential prediction of sub-figure (b) is well fitted, and the point distribution is compact, indicating that the model can effectively describe the changing trend of the material potential energy distribution on the gas, liquid, and solid multiphase interface, confirming the applicability of the Fick-interface resistance coupling method. The predicted values of oxygen and water fluxes in sub-figure (c) are highly consistent

with the measured values, with a high R^2, indicating that the constructed mass transfer model has a high explanatory power for gas/liquid migration in the dark tea fermentation bed environment, especially for scenes with complex three-phase interface structures. The enthalpy change prediction effect of sub-graph (d) is relatively ideal, but some scattered points slightly deviate from the reference line, indicating that the energy release modeling may have nonlinear errors in the local high activity stage or be affected by the complex metabolic heat release process. The Gibbs free energy transformation, chemical potential gradient, oxygen/water mass transfer flux, and reaction enthalpy change R^2 of the dark tea solid-state fermentation process are greater than 0.9, and the goodness of fit is good.

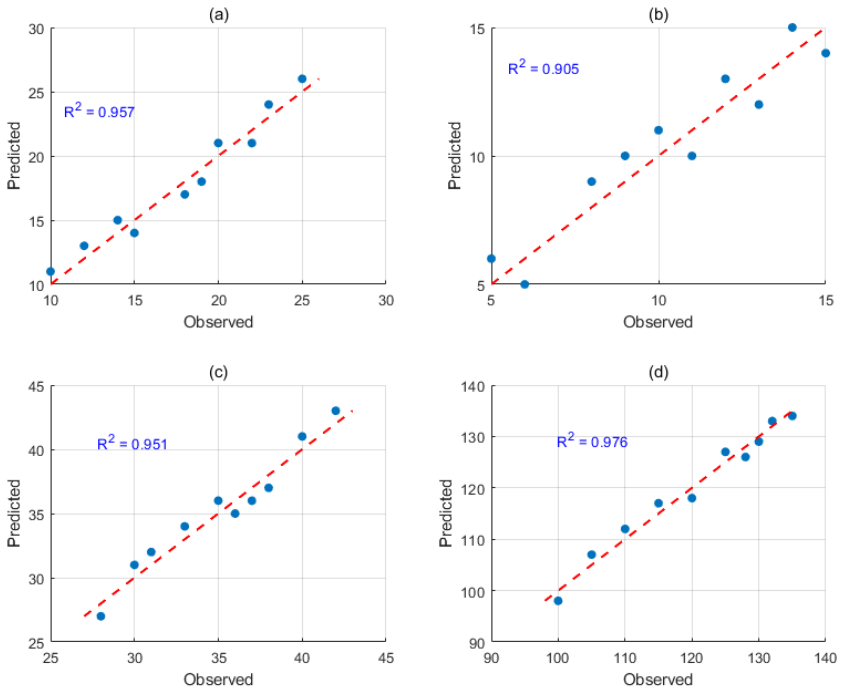

Fig. 3: Fitting evaluation

(a) Gibbs free energy transformation fitting evaluation

(b) Chemical potential gradient fitting evaluation

(c) Oxygen/water mass transfer flux fitting evaluation

(d) Reaction enthalpy change fitting evaluation

The structural equation model contains 3 latent variables and 12 observed variables, with 48 degrees of freedom. The number of independent samples participating in the model fitting is 45, and the ratio of observed variables to sample size is 1:3.75, satisfying the empirical criterion that each observed variable corresponds to at least 3 to 5 samples in structural equation model analysis. Model parsimony was evaluated by comparing the parsimony-normalized fit index and the parsimony-normalized fit index. The parsimony-normalized fit index was 0.93, while the parsimony-normalized fit index was 0.71. The latter is greater than the recommended threshold of 0.6, indicating that the model achieves a reasonable balance between goodness of fit and the number of parameters, and does not show a significant tendency for overparameterization.

Microecological Response Prediction Capability

Environmental parameters (such as temperature, humidity, gas concentration) and microbial community structure data are collected at different stages of the dark tea solid-state fermentation process. Environmental parameters and microbial functional indicators are preprocessed and screened to construct an input feature set for predicting the dynamic changes of microbial communities. The environmental characteristics are used as input, and the microbial community change indicators

DOI: 10.3844/ajbbsp.2026.22.03.034

are used as output for model training. The k-fold cross-validation method (5 folds) is used to divide the data into a training set and a validation set to evaluate the generalization ability of the model under different data partitions. The prediction error (mean square error) on each fold of the validation set is calculated, and the error data of each fold is collected.

Figure 4 shows the distribution of the prediction errors of the model in the 5-fold cross-validation. The errors of each fold are roughly between 0.13 and 0.21, indicating that the overall prediction error of the model is low and stable. Most of the prediction errors are concentrated, and the model has good consistency. The high-precision prediction ability of the model for the dynamic changes of the microbial community is verified (the cross-validation accuracy rate exceeds 79%), supporting the application potential of the model in the actual fermentation environment regulation. The reported goodness-of-fit and cross-validation results are based on a dataset of 45 independent fermentation samples. The model outputs may be sensitive to parameterization choices, and the limited dataset size constrains the assessment of model robustness under broader conditions.

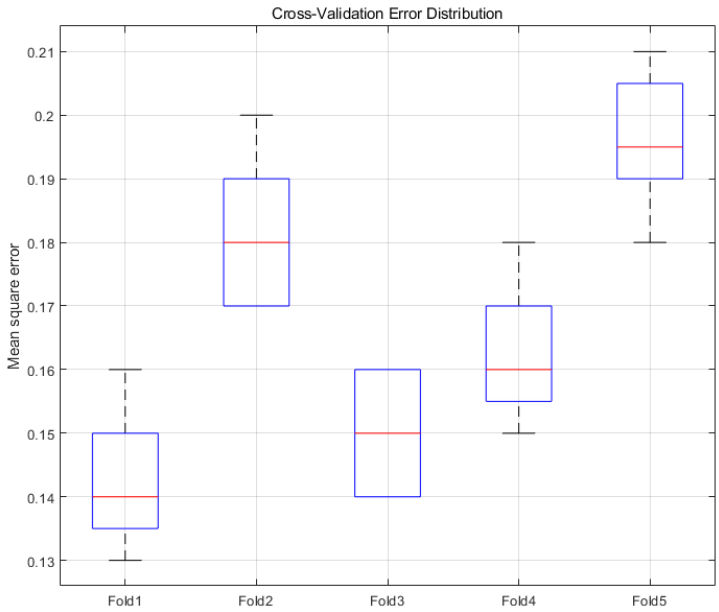

Fig. 4: 5-Fold cross-validation

Test of the Correlation between Thermodynamic Fitness and Community Function

The calculation is based on the metabolic reaction pathway of the dominant microorganisms in the fermentation process (obtained by 16S/ITS sequencing and functional prediction), combined with the standard free energy data of known reactants and products, and corrected by the measured values of the free energy data under actual concentration conditions according to the Nernst equation. The concentration gradient of key substances such as oxygen, water, and ammonia at the gas, liquid, and solid interfaces is modeled, and the overall energy release level is estimated based on the standard enthalpy change values of the main reactions in the literature data, combined with the fermentation reaction rate and conversion rate. The 16S rRNA and ITS sequences at multiple time points are quality-controlled and OTU (Operational Taxonomic Unit) clustered, and the potential functional gene distribution of each sample microbial community is predicted to extract key functional modules (carbon metabolism, nitrogen metabolism, fermentation, and amino acid metabolism). Thermodynamic parameters (free energy transformation ΔG, chemical potential gradient μ, reaction enthalpy change ΔH) are paired with the abundance or expression intensity of functional modules in different samples to construct a 3×4 correlation coefficient matrix.

Figure 5 shows the Pearson correlation coefficient between thermodynamic parameters and microbial metabolic functional modules. The vertical axis represents three thermodynamic indicators, including Gibbs Free Energy, Chemical Potential, and Enthalpy Change. The horizontal axis represents four typical microbial metabolic functional modules: Carbon Metabolism, Nitrogen Metabolism, Fermentation, and Amino Acid Metabolism. ΔG shows a high correlation with Carbon Metabolism (0.85),

DOI: 10.3844/ajbbsp.2026.22.03.034

indicating a statistical association between free energy transformation and the carbon metabolism functional module. The positive correlation coefficient between μ and Nitrogen Metabolism is 0.7, suggesting an association between the chemical potential gradient and nitrogen metabolism. The correlation coefficient between ΔH and Fermentation is 0.9, reflecting a strong statistical relationship between reaction enthalpy change and the fermentation module. ΔH shows a negative correlation with Amino Acid Metabolism (-0.5). These correlations are derived from integrated modeling and statistical associations. They are interpreted as reflecting potential thermodynamic constraints on metabolic pathways rather than direct evidence that more favorable ΔG′ values drive the ecological success of specific microbial groups.

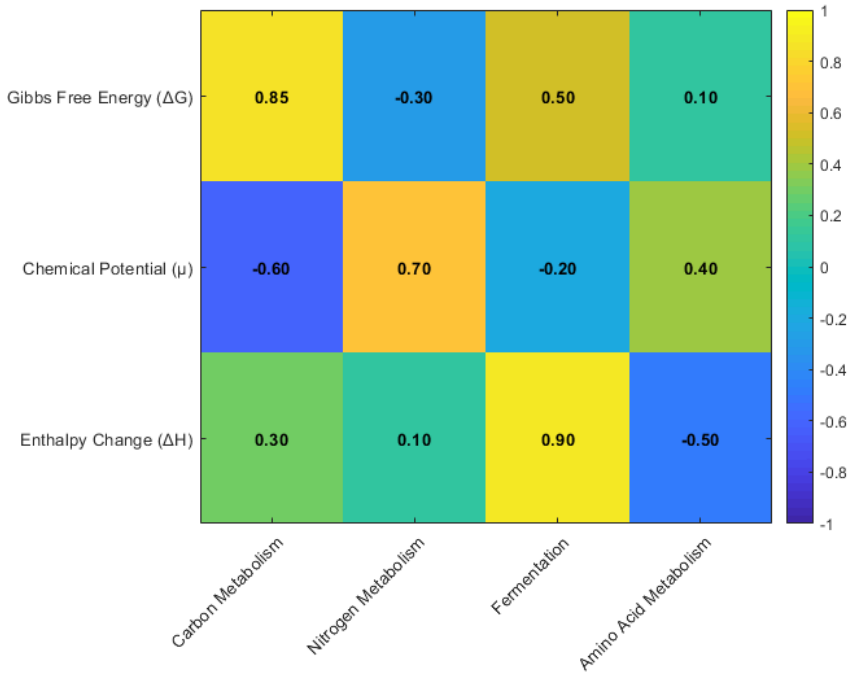

Fig. 5: Correlation coefficient

Systemic Responses of Microbial Community Structure and Function

Dark tea fermentation samples with different ratios are prepared: sample 1, 100% tea leaves; sample 2, 90% tea leaves + 10% auxiliary materials; sample 3, 85% tea leaves + 15% auxiliary materials. At least 3 biological replicates are prepared for each ratio. Solid-state fermentation is carried out according to the established fermentation conditions (temperature, humidity, inoculated strains). Sampling is performed at the set time point (21 days) after fermentation. Total microbial DNA is extracted from each sample using an appropriate DNA extraction kit. DNA quality and concentration are measured to ensure that they meet sequencing requirements. The samples are sent to the Illumina MiSeq platform to obtain sequence data for each sample. Sequence quality control, splicing, and denoising are performed. The relative abundance of core strains in each sample is calculated.

Figure 6 shows the relative abundance differences of the five core microorganisms in different fermentation samples, namely sample 1: 100% tea, sample 2: 90% tea + 10% auxiliary materials, and sample 3: 85% tea + 15% auxiliary materials. The X-axis represents different fermentation samples, representing different raw material ratios. The Y-axis represents the relative abundance of each core microorganism in the sample (in the range of 0-0.5). Different colors in the bar chart correspond to five species: Lactobacillus, Saccharomyces, Aspergillus, Bacillus, and Streptomyces. Lactobacillus is the most abundant in sample 3 (about 35%), which may indicate that the addition of auxiliary materials is conducive to the growth of Lactobacillus and enhances the production of sour taste. Lactobacillus and yeast have the highest relative abundance in sample 2 (about 25%), indicating that moderate auxiliary materials are conducive to yeast metabolic activity and promote the production of aroma substances. Aspergillus is slightly higher in sample 3 than in the other samples, which may promote the decomposition of polysaccharides. Bacillus is more abundant in sample 2, which is helpful for protein degradation and the release of flavor substances. Streptomyces is less abundant, but slightly increases in sample 2, which may assist in the degradation of complex organic matter.

DOI: 10.3844/ajbbsp.2026.22.03.034

High-quality fresh leaf black tea raw materials are collected, cleaned, dried, and set aside. Auxiliary materials (red yeast rice, wheat bran) are prepared and weighed according to the predetermined ratio (100:10, 100:15, 100:20) for later use. The black tea leaves are mixed with the auxiliary materials to ensure the accuracy of the ratio. The mixed fermentation raw materials are divided into 3 groups, named Group A, B, and C. Group A: natural fermentation (no exogenous strains are added, relying on natural inoculation of environmental microorganisms), and the auxiliary material ratio is (100:10). Group B: Inoculation of a single strain (Saccharomyces cerevisiae), the inoculation amount is 1% of the total mass of the fermentation, and the auxiliary material ratio is (100:15). Group C: Inoculating composite bacteria (such as lactic acid bacteria, yeast and mold mixed strains), the total inoculation amount is 2% of the total mass of the fermentation, and the auxiliary material ratio is prepared (100:20). The three groups are placed in fermentation containers and set different conditions: humidity control: Group A 60%±2%, Group B 65%±2%, Group C 70%±3%. Temperature control: Group A 30°C±1°C, Group B 28°C±1°C, Group C 32°C±1°C. Ventilation and compost turning frequency: Group A compost is turned twice a day with good ventilation. Group B compost is turned once a day with less ventilation. Group C compost is turned three times a day with intermittent ventilation to ensure sufficient oxygen. The fermentation cycle is set to 10 days. Samples are collected once a day (a total of 11 time points, including 0 days before fermentation). Temperature and humidity environmental parameters are recorded during sampling. Samples are collected for subsequent microbial diversity sequencing analysis and chemical composition detection.

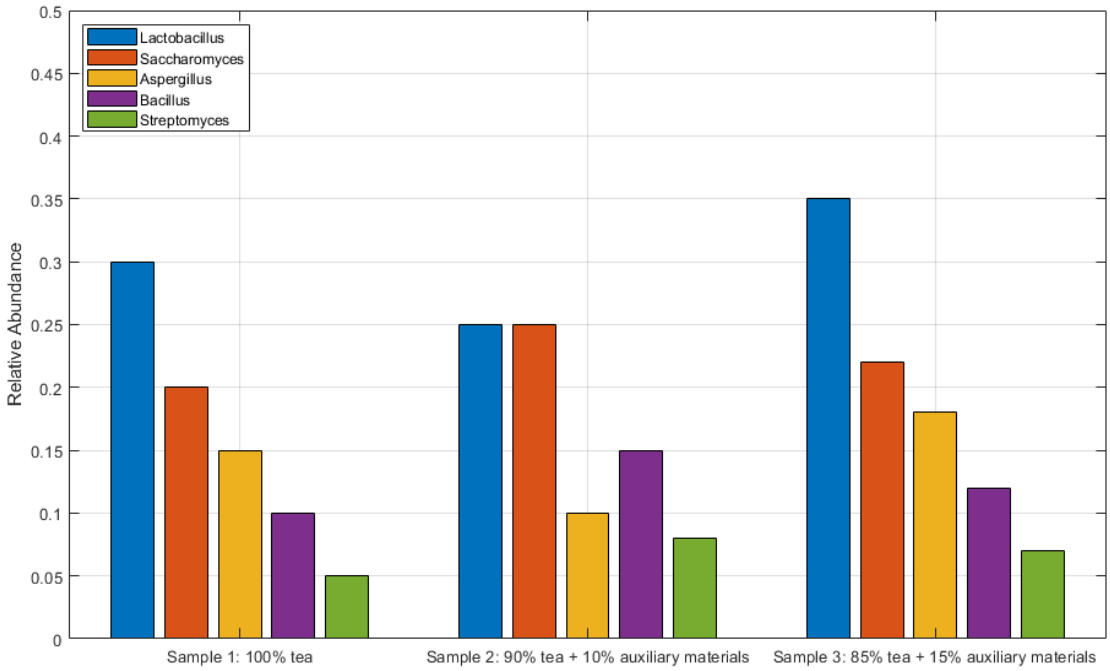

Fig. 6: Relative abundance differences

The horizontal axis of Figure 7 represents the time course of the fermentation process, from day 0 (start of fermentation) today 10. The vertical axis represents the Shannon index, which is an indicator of the alpha diversity of the microbial community. Group A denotes natural fermentation with an auxiliary material ratio of 100:10, Group B denotes single-strain inoculation with an auxiliary material ratio of 100:15, and Group C denotes composite-strain inoculation with an auxiliary material ratio of 100:20. The larger the value, the richer and more uniform the community. Group C has the highest overall diversity and grows faster, indicating that the treatment promotes community richness. Group B has relatively low diversity and grows slowly, which may indicate that community development is limited. Group A is between the two, showing a certain increase in diversity.

The proposed energy cascade regulatory interpretation is supported by a systematic integration of multi-dimensional data. At the level of mass migration, the mass transfer fluxes of oxygen and water show a high degree of consistency between model calculations and measured values, and their spatial gradient distribution corresponds quantitatively to the spatial location of dominant species in the microbial community. At the thermodynamic level, changes in Gibbs free energy of different

DOI: 10.3844/ajbbsp.2026.22.03.034

metabolic pathways are correlated with changes in the abundance of corresponding functional genes, with metabolic pathways releasing larger amounts of free energy exhibiting higher node degree and betweenness centrality in network analysis. At the community response level, structural equation modeling indicates that energy state serves as a mediating variable in the association between mass migration and microecological succession, with its indirect effect accounting for over 60% of the total effect. As the evidence presented here is derived from integrated modeling and statistical associations rather than perturbation experiments, the synergistic changes in multi-source data over time series and the statistical significance in the path model collectively support an inferred cascade relationship from macroscopic mass transfer gradients to microscopic metabolic energy states and then to community structure remodeling.

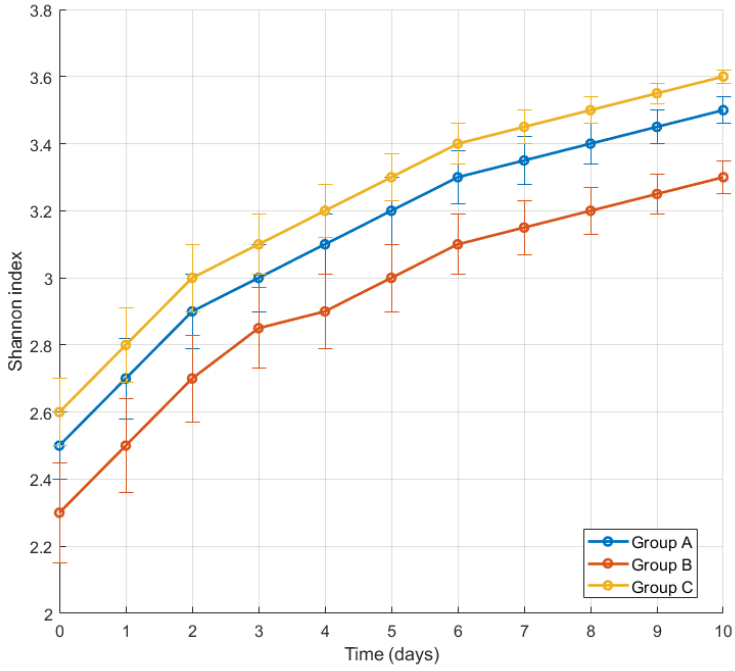

Fig. 7: A diversity

Conclusion

This paper focuses on the synergistic relationship between material migration, thermodynamic constraints, and microecological succession during the solid-state fermentation of dark tea and constructs a multiphase, thermodynamic, and microecological coupling modeling system. The migration behavior of key substances is described by Fick's diffusion law and interfacial resistance theory, and the thermodynamic feasibility of microbial energy metabolism is evaluated by combining Gibbs free energy and KEGG metabolic pathways. High-throughput sequencing and structural equation models are further used to quantify community succession paths and synergistic associations. The results suggest that oxygen and water migration are associated with metabolic energy status, and that energy regulation plays a role in community evolution, offering an interpretation for the formation mechanism of dark tea quality. It is emphasized that these findings are based on integrated modeling and statistical correlations, and do not independently demonstrate direct causal mechanisms. Although this study achieves a high resolution at the descriptive level, there are still limitations in spatial hierarchical modeling and community function verification. Future integration of multi-scale real-time monitoring and multi-omics experiments will further improve modeling accuracy and predictive capability. This model provides a quantifiable theoretical tool for optimizing the process and controlling the quality of solid-state fermentation of dark tea. Through the quantitative relationship between mass transfer flux and thermodynamic parameters in the model, the temperature, humidity, and ventilation conditions during fermentation are parametrically designed to determine the optimal process window for maintaining microbial metabolic activity and energy efficiency. All claims presented in this study are confined to the dark tea solid-state fermentation system described herein. Broader generalization to other fermentation systems would require independent experimental validation.

The coupled model constructed in this study provides a systematic description of the relationship between mass transfer, thermodynamics, and microecology at the mechanistic level. However, it still employs a one-dimensional diffusion approximation and a quasi-steady-state assumption in the spatial dimension, failing to fully analyze the spatial heterogeneity characteristics caused by differences in temperature, moisture, and oxygen distribution within the fermentation stack. Furthermore, it does not incorporate short-term fluctuations in the local microenvironment into the model framework. In actual solid-state fermentation, the microenvironment of the microbial community exhibits a significantly non-uniform spatial distribution and undergoes rapid changes under process interventions such as turning and ventilation. The regulatory effects of these factors on community structure and metabolic function are not fully reflected in the current model. Future research will combine multi-scale sensing technology and explicit spatial modeling methods to introduce the non-uniform distribution of local mass transfer coefficients and thermodynamic parameters into a three-dimensional spatial grid, constructing a high-resolution model that reflects the dynamic evolution of the microenvironment within the stack, thereby improving the predictive ability for the spatiotemporal heterogeneity of the fermentation process.

This study focuses on the solid-state fermentation of dark tea as a specific multiphase system, constructing a ternary coupling model of mass migration, thermodynamic constraints, and microecological succession. Model fitting and validation were based on experimental data collected from the same solid-state fermentation system under conditions of a single raw material source, fixed fermentation container, and standard process parameters. The high goodness of fit and prediction accuracy Reflect the effectiveness and reliability of the model within the experimental system described in this study. The explanation of the coupling mechanism in this study is based on statistical inferences and structural equation model analysis results supported by the current experimental data. Extension to other solid-state fermentation systems should be based on experimental validation within the corresponding systems.

Acknowledgment

Thank you to the publisher for their support in the publication of this research article. We are grateful for the resources and platform provided by the publisher, which have enabled us to share our findings with a wider audience. We appreciate the efforts of the editorial team in reviewing and editing our work, and we are thankful for the opportunity to contribute to the field of research through this publication.

Funding Information

Foundation projects: The Natural Science Foundation’s regional joint fund project of Hunan Province (2023JJ50338); Yiyang City science and technology innovation plan project 2023.

Author’s Contributions

Zhanjun Liu: Designed the research study, wrote the manuscript.
Jiawei Sun: Designed the research study.
Taotao Li, Zhiyuan Hu, and Shiquan Liu: Analyzed the data.
All authors contributed to editorial changes in the manuscript. All authors read and approved the final manuscript.

Ethics

This article is original and contains unpublished material. The corresponding author confirms that all of the other authors have read and approved the manuscript and no ethical issues involved.

References

1. Dai, Y., Liu, Y., LI, Y., Li, Q., Liu, Z., Zhang, T., Yang, T., Fang, S., Zhang, B., & Pan, K. (2024). Solid-State Fermentation of Ganoderma lucidum on the Soluble Sugar Metabolism of Three Summer-Autumn Black Tea Varieties. Journal of Food Processing and Preservation, 2024, 1–18. https://doi.org/10.1155/2024/8856934
2. Saad, M. M., Saad, A. M., Hassan, H. M., Ibrahim, E. I., Abdelraof, M., & Ali, B. A. (2023). Optimization of tannase production by Aspergillus glaucus in solid-state fermentation of black tea waste. Bioresources and Bioprocessing, 10(1), 73. https://doi.org/10.1186/s40643-023-00686-9

3. Jiang, J., Zhang, M., An, T., Zu, Z., Song, P., Chen, M., Yue, P., & Gao, X. (2022). Preparation of instant dark tea by liquid-state fermentation using sequential inoculation with Eurotium cristatum and Aspergillus niger: Processes optimization, physiochemical characteristics and antioxidant activity. LWT, 162, 113379. https://doi.org/10.1016/j.lwt.2022.113379
4. An, T., Shen, S., Zu, Z., Chen, M., Wen, Y., Chen, X., Chen, Q., Wang, Y., Wang, S., & Gao, X. (2023). Changes in the volatile compounds and characteristic aroma during liquid-state fermentation of instant dark tea by Eurotium cristatum. Food Chemistry, 410, 135462. https://doi.org/10.1016/j.foodchem.2023.135462
5. An, T., Chen, M., Zu, Z., Chen, Q., Lu, H., Yue, P., & Gao, X. (2021). Untargeted and targeted metabolomics reveal changes in the chemical constituents of instant dark tea during liquid-state fermentation by Eurotium cristatum. Food Research International, 148, 110623. https://doi.org/10.1016/j.foodres.2021.110623
6. Sun, H., Fan, R., Fang, R., Shen, S., Wang, Y., Fu, J., Hou, R., Sun, R., Bao, S., Chen, Q., Yue, P., & Gao, X. (2024). Dynamics changes in metabolites and pancreatic lipase inhibitory ability of instant dark tea during liquid-state fermentation by Aspergillus niger. Food Chemistry, 448, 139136. https://doi.org/10.1016/j.foodchem.2024.139136
7. Feng, X., Chen, M., Song, H., Ma, S., Ou, C., Li, Z., Hu, H., Yang, Y., Zhou, S., Pan, Y., Fan, F., Gong, S., Chen, P., & Chu, Q. (2023). A systemic review on Liubao tea: A time-honored dark tea with distinctive raw materials, process techniques, chemical profiles, and biological activities. Comprehensive Reviews in Food Science and Food Safety, 22(6), 5063–5085. https://doi.org/10.1111/1541-4337.13254
8. Zou, Y., Zhang, Y., Tian, Y., Liu, M., Yuan, Y., Lai, Y., Liu, X., Xu, W., Tan, L., Tang, Q., Li, P., & Xu, J. (2022). Microbial Community Analysis in Sichuan South-road Dark Tea Piled Center at Pile-Fermentation Metaphase and Insight into Organoleptic Quality Development Mediated by Aspergillus niger M10. Frontiers in Microbiology, 13, 930477. https://doi.org/10.3389/fmicb.2022.930477
9. Li, Y., Hao, J., Zhou, J., He, C., Yu, Z., Chen, S., Chen, Y., & Ni, D. (2022). Pile-fermentation of dark tea: Conditions optimization and quality formation mechanism. LWT, 166, 113753. https://doi.org/10.1016/j.lwt.2022.113753
10. Chen, Q., Zhang, M., Chen, M., Li, M., Zhang, H., Song, P., An, T., Yue, P., & Gao, X. (2021). Influence of Eurotium cristatum and Aspergillus niger individual and collaborative inoculation on volatile profile in liquid-state fermentation of instant dark teas. Food Chemistry, 350, 129234. https://doi.org/10.1016/j.foodchem.2021.129234
11. Peña-Lucio, E., Chávez-González, M., Londoño-Hernandez, L., Ruiz, H., Martínez-Hernandez, J., Govea-Salas, M., Sukumaran, P. N., Abdulhameed, S., & Aguilar, C. (2023). Solid-State Fermentation of Green Tea Residues as Substrates for Tannase Production by Aspergillus niger TBG 28A: Optimization of the Culture Conditions. Fermentation, 9(9), 781. https://doi.org/10.3390/fermentation9090781
12. Pang, Y., Wei, Y., Wei, K., Huang, R., Peng, L., Zhu, Y., & Wei, X. (2024). A Rising Star in Dark Teas: The Processing, Microorganisms, Chemicals, Bioactivities, and Safety of Qingzhuan Tea. ACS Food Science & Technology, 4(4), 796–812. https://doi.org/10.1021/acsfoodscitech.3c00630
13. Huang, Y., Chen, R., Chen, Y., Ho, C.-T., Hou, A., Zhang, X., Zhu, M., Zhang, C., Wang, Y., Liu, Z., & Xiao, Y. (2023). Dynamics changes in volatile profile, non-volatile metabolites and antioxidant activities of dark tea infusion during submerged fermentation with Eurotium cristatum. Food Bioscience, 55, 102966. https://doi.org/10.1016/j.fbio.2023.102966
14. Xu, W., Zhao, Y., Jia, W., Liao, S., Bouphun, T., & Zou, Y. (2023). Reviews of fungi and mycotoxins in Chinese dark tea. Frontiers in Microbiology, 14, 1120659. https://doi.org/10.3389/fmicb.2023.1120659
15. Lasinskas, M., Jariene, E., Vaitkeviciene, N., Kulaitiene, J., Adamaviciene, A., & Hallmann, E. (2023). The Impact of Solid-Phase Fermentation on Flavonoids, Phenolic Acids, Tannins and Antioxidant Activity in Chamerion angustifolium (L.) Holub (Fireweed) Leaves. Plants, 12(2), 277. https://doi.org/10.3390/plants12020277
16. Shen, S., Fu, J., Fan, R., Zhang, J., Sun, H., Wang, Y., Ning, J., Yue, P., Zhang, L., & Gao, X. (2024). Changes in the key odorants of loose-leaf dark tea fermented by Eurotium cristatum during aging for one year: Focus on the stale aroma. Food Research International, 197, 115244. https://doi.org/10.1016/j.foodres.2024.115244
17. Xinhui, W. U., Jinjie, D. U., Xiaochun, L. I. U., Kaibin, L., Yuna, Q., Weijie , L., Lingzhi, Z., Zhirong, L., & Ruijin, Q. (2024). Screening of Fungal Strains for Single-Culture Solid-State Fermentation of Liupao Tea. Food Science, 45(6), 64–71. https://doi.org/10.7506/spkx1002-6630-20230608-075
18. Ma, W., Zhu, Y., Shi, J., Wang, J., Wang, M., Shao, C., Yan, H., Lin, Z., & Lv, H. (2021). Insight into the volatile profiles of four types of dark teas obtained from the same dark raw tea material. Food Chemistry, 346, 128906. https://doi.org/10.1016/j.foodchem.2020.128906
19. Huang, J., Li, Y., Zhang, S., Zou, Y., Zheng, Q., Lin, J., & Guo, L. (2022). Amelioration effect of water extract from Ganoderma resinaceum FQ23 solid-state fermentation fungal substance with high-yield ergothioneine on anxiety-like insomnia mice†. Food & Function, 13(24), 12925–12937. https://doi.org/10.1039/d2fo01847k
20. Chen, Q., Zhu, Y., Liu, Y., Liu, Y., Dong, C., Lin, Z., & Teng, J. (2022). Black tea aroma formation during the fermentation period. Food Chemistry, 374, 131640. https://doi.org/10.1016/j.foodchem.2021.131640
21. Huang, X., Li, Y., Zhou, F., Xiao, T., Shang, B., Niu, L., Huang, J., Liu, Z., Wang, K., & Zhu, M. (2024). Insight into the chemical compositions of Anhua dark teas derived from identical tea materials: A multi-omics, electronic sensory, and microbial sequencing analysis. Food Chemistry, 441, 138367. https://doi.org/10.1016/j.foodchem.2024.138367
22. Xu, W., Zhu, Y., Lin, L., Tunyaluk, B., & Li, P. (2024). Dynamic changes in volatile components during dark tea wine processing. LWT, 194, 115783. https://doi.org/10.1016/j.lwt.2024.115783
23. Xiao, Y., Huang, Y., Chen, Y., Fan, Z., Chen, R., He, C., Li, Z., & Wang, Y. (2021). Effects of Solid-State Fermentation with Eurotium cristatum YL-1 on the Nutritional Value, Total Phenolics, Isoflavones, Antioxidant Activity, and Volatile Organic Compounds of Black Soybeans. Agronomy, 11(6), 1029. https://doi.org/10.3390/agronomy11061029
24. Chen, L., Wang, H., Ye, Y., Wang, Y., & Xu, P. (2023). Structural insight into polyphenol oxidation during black tea fermentation. Food Chemistry: X, 17, 100615. https://doi.org/10.1016/j.fochx.2023.100615
25. Zhu, W., Wang, W., Xu, W., Wu, S., Chen, W., Huang, Y., & Wang, S. (2022). Influence of thermophilic microorganism on non-volatile metabolites during high-temperature pile-fermentation of Chinese dark tea based on metabolomic analysis. Food Science and Biotechnology, 31(7), 827–841. https://doi.org/10.1007/s10068-022-01098-9

26. Du, J., Li, X., Liu, N., Wang, Y., Li, Y., Jia, Y., An, X., & Qi, J. (2024). Improving the quality of Glycyrrhiza stems and leaves through solid-state fermentation: flavonoid content, antioxidant activity, metabolic profile, and release mechanism. Chemical and Biological Technologies in Agriculture, 11(1), 105. https://doi.org/10.1186/s40538-024-00631-8
27. Huang, C.-H., Liao, Y.-M., & Tsai, G.-J. (2024). Solid-State Fermentation of Grain-Derived By-Products by Aspergillus kawachii and Rhizopus oryzae: Preparation and Evaluation of Anti-Allergic Activity. Fermentation, 10(9), 457. https://doi.org/10.3390/fermentation10090457
28. Cerda-Cejudo, N. D., Buenrostro-Figueroa, J. J., Sepúlveda-Torre, L., Torres-León, C., Chávez-González, M. L., Ascacio-Valdés, J. A., & Aguilar, C. N. (2023). Solid-State Fermentation for the Recovery of Phenolic Compounds from Agro-Wastes. Resources, 12(3), 36. https://doi.org/10.3390/resources12030036
29. Li, Y., Xu, L., & Guo, S. (2023). Effects of Solid-State Fermentation with the Ganoderma spp. and Coriolus versicolor on the Total Phenol Contents and Antioxidant Properties on Black Soybean. Journal of Chemistry, 2023, 1–8. https://doi.org/10.1155/2023/9462748
30. Nayab, D.-, Akhtar, S., Bangash, N., Nisa, W.-, Hayat, M. T., Zulfiqar, A., Niaz, M., Qayyum, A., Syed, A., Bahkali, A. H., & Elgorban, A. M. (2022). Production of Glucoamylase from Novel Strain of Alternaria Alternata under Solid State Fermentation. BioMed Research International, 2022(1), 2943790. https://doi.org/10.1155/2022/2943790